Metabolic Effects and Biomarkers Identification on Nicotine-induced Intrauterine Growth Retardation with NMR-based metabonomic strategy

Jianghua Feng[1]

[1]*Department of Electronic Science, Fujian Key Laboratory of Plasma and Magnetic Resonance, Xiamen University, Xiamen, Fujian, China, People's Republic of*

Background: There is consistent evidence to relate maternal harmful lifestyle such as smoking cigarettes, drink alcohol or abuse drug to an increase risk of intrauterine growth retardation, however, the definite mechanisms governing pregnancy smoking exposure and IUGR risk are still keep unclear. In another side, it is quite necessary and important to establish a safe, convenient, specific and early diagnostic procedure for IUGR due to the inherent defects of the present diagnostic methods.

Methods: Pregnant Wistar rats were intragastrically administered with different doses of nicotine (0.5, 1.0 and 2.0 mg/kg) daily from gestational day (GD) 11. At GD20, all the samples including fetal plasma, amniotic fluid and maternal plasma were collected. The other pregnant rats as those described above were subject to 2.0 mg/kg of nicotine daily gavages from GD9, the samples of maternal plasma were collected at GD11, GD14, GD17 and GD20, respectively. NMR-based metabonomic approaches in combination with multivariate statistical analysis have been used to analyze the metabolic responses of those biofluids to nicotine-induced dose- and time-dependent effects in order to demonstrate alteration of intrauterine metabolism and to identify the potential biomarkers in maternal blood served to early diagnosis of IUGR.

Results and discussion: The IUGR rates of fetuses in nicotine-treated groups were significantly augmented compared with that in control group. The wealth of information from metabonomics analysis has revealed different metabolic profiling in the respective pathophysiological regime including maternal plasma, fetal plasma and amniotic fluids (Figs. 1&2). The metabolic changes due to nicotine-administration involved abnormal glucose, lipid and protein metabolisms which were characterized by the variations in concentrations of a collection of metabolites in fetal and maternal plasma and amniotic fluid of IUGR (Fig. 3). Further, some metabolites were selected from maternal plasma as biomarker candidates served to the diagnosis of nicotine-induced IUGR.

Conclusions: NMR-based metabonomics appears as a promising approach for distinguishing the development of IUGR, and a collection of candidate biomarkers in maternal plasma are identified for the diagnosis of early IUGR. And further, such information could be served to prevention and therapy of IUGR in the clinical practice.

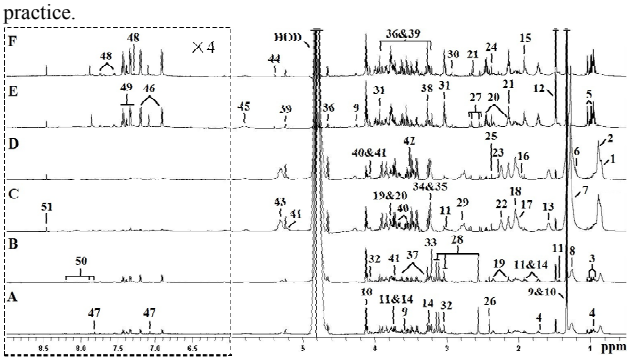

Figure 1. Representative 600 MHz water-suppressed ^{1}H NMR spectra (δ0.5-6.0 and δ6.0-9.0) of fetal rat plasma (A and B), pregnant rat plasma (C and D) and rat amniotic fluids (E and F) from control (A, C and E) and (B, D and F) high-dosage nicotine groups. Keys: 1, LDL, C$\underline{H}_3$-(CH$_2$)$_n$-; 2, VLDL, C$\underline{H}_3$-(CH$_2$)$_n$-; 3, isoleucine; 4, leucine; 5, valine; 6, 3-hydroxybutyrate; 7, LDL, CH$_3$-(C$\underline{H}_2$)$_n$-; 8, VLDL, CH$_3$-(C$\underline{H}_2$)$_n$-; 9, threonine; 10, lactate; 11, lysine; 12, alanine; 13, VLDL, -C$\underline{H}_2$-CH$_2$-C=O; 14, arginine; 15, acetate; 16, Lipid, -C$\underline{H}_2$-CH$_2$-CH=CH-; 17, Lipid, -C$\underline{H}_2$-CH=CH-; 18, N-Acetyl Glycoprotein; 19, glutamate; 20, glutamine; 21, methionine; 22, Lipid, -C$\underline{H}_2$-C=O; 23, acetone; 24, acetoacetate; 25, pyruvate; 26, succinate; 27, citrate; 28, Ca-&Mg-EDTA^{2-}; 29, Lipid, =CH-C$\underline{H}_2$-CH=; 30, trimethylamine; 31, creatine; 32, creatinine; 34, phophocholine; 35, glycerophosphocholine; 36, β-Glucose; 37, EDTA; 38, TMAO; 39, α-Glucose; 40, *myo*-inositol; 41, glycerol; 42, glycine; 43, Lipid, -CH=CH-; 44, allantoin; 45, urea; 46, tyrosine; 47, histidine; 48, tryptophan; 49, phenylalanine; 50, nocotinate; 51, formate.

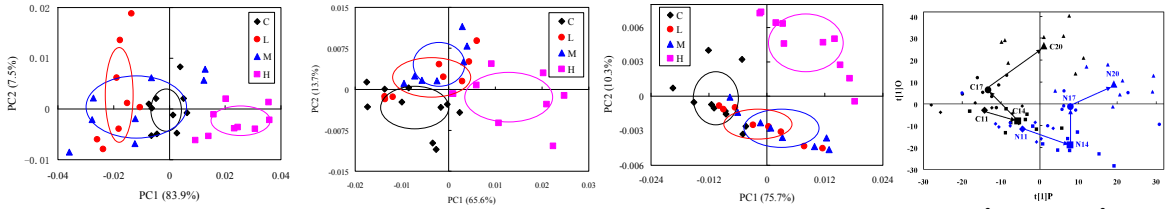

(A) (B) (C) (D) Q^2X=76.8%, Q^2=0.331

Figure 2. PCA scores plot based on (A) CPMG ^{1}H NMR spectra of pregnant rat plasma, (B) CPMG ^{1}H NMR spectra of fetal rat plasma, and (C) NOESYPR1D ^{1}H NMR spectra of rat amniotic fluids following the treatment of different-dosage nicotine. C (control group, black diamond ♦), L (low-dosage group, red dot ●), M (medium-dosage group, blue triangle ▲) and H (high-dosage group, pink dot ■). The center of each ellipse indicates the mean, and the margin indicates one standard deviation. (D) OPLS-DA scores plot based on NOESYPR1D ^{1}H NMR spectra of pregnant rat plasma following the treatment of nicotine. C11 (♦Day 11), C14 (■Day 14), C17 (●Day 17) and C20 (▲Day 20) post-pregnancy in control group (black marks); N11 (♦Day 11), N14 (■Day 14), N17 (●Day 17) and N20 (▲Day 20) post-pregnancy in nicotine group (blue marks). The big marks indicate the mean in each time point. C, Control group; N, Nicotine group.

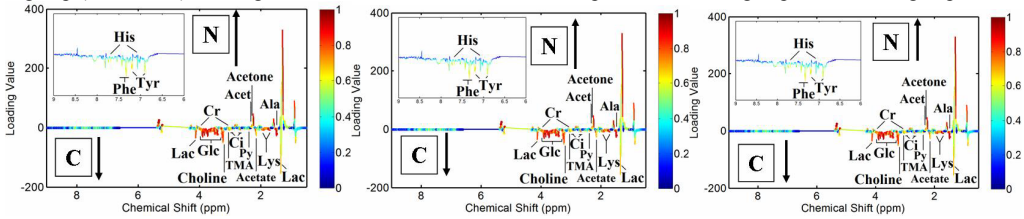

(A) (B) (C)

Figure 3. OPLS-DA scores derived from ^{1}H NMR spectra of (A) pregnant rat plasma, (C) fetal rat plasma and (E) rat amniotic fluids and corresponding coefficient plots (B), (D) and (F) obtained from control and nicotine-dosed groups. C, Control group; N; High-dosage nicotine group. The color map shows the significance of metabolites variations between the two classes. Peaks in the positive direction indicate metabolites that are more abundant in the dosed groups. Consequently, metabolites that are more abundant in the control group are presented as peaks in the negative direction.

Acknowledgement: This work was partially supported by Fundamental Research Funds for the Central Universities (2011121046).

References

1. Kalinka J, et al. *Am. J. Perinatol.*, 25(2005): 41-47.
2. Kamleh MA, et al. *Curr. Pharm. Biotechno.*, 12(2011): 976-995.
3. Nicholson JK, et al. *Anal. Chem.*, 67(1995) : 793-811.